

AN ANALYTICAL STUDY ON PERFORMANCE CHARACTERISTICS OF A ROTATING HEAT PIPE

Jong Hoon Jang and Jae Dong Choi*
School of Mechanical Engineering

<Abstract>

An analytical study is conducted for the performance characteristics of a rotating heat pipe. The complete Navier-Stokes and energy equations are transformed to a set of ordinary differential equations by introducing new variables. Numerical results are obtained for various Pr numbers by using the Runge-Kutter method. The velocity profiles, temperature distributions, layer thickness, and heat transfer are calculated. The parametric study is conducted to find the effects of various design factors. The properties of the working fluid, the rotating speed, and the taper angle greatly affect the performance of the rotating heat pipe. The results show that the increase in the rotating speed and taper angle enhances the heat transport capability.

회전형 히트파이프의 성능 특성에 대한 해석적 연구

장종훈 · 최제동*
기계공학부

<요 약>

본 논문에서는 회전형 히트파이프의 성능 특성에 대한 해석적 연구가 수행되었다. 편미분방정식 형태의 Navier-Stokes 식과 에너지 방정식을 새로 설정된 변수를 사용하여 미분

* Graduate student

방정식으로 변환시키고 Runge-Kutter 방법을 이용하여 여러 값의 Pr수 대하여 응축액의 속도분포, 온도분포, 두께 및 열전달량을 계산하였다. 또 몇 가지의 주요 설계변수 즉 작동 유체의 성질, 회전속도, 응축부 내벽의 경사각도가 회전형 히트파이프의 성능에 미치는 영향에 대한 연구 결과를 얻었으며 회전속도 및 경사각도의 증가는 회전형 히트파이프의 열전달 능력을 증가 시키는 경향을 나타냈다.

1. Introduction

Heat pipes are very effective devices to transport a large amount of heat energy using the phase change of the working fluid[1,2]. Therefore heat pipes have been used for various applications since they were introduced. A rotating heat pipe are also one type of heat pipes, but its wick structure to return the condensate from the condenser to the evaporator is different from that of heat pipes. The rotating heat pipe is consisted of a hollow, taper pipe sealed at both ends and some working fluid without the wick structure. Thus the rotating heat pipe can be used to transport heat from/to the some rotating parts. A clear application of the rotating heat pipe is to cool the high speed induction motor. The rotating heat pipe is built into the shaft to cool the rotor.

A system to be considered is schematically shown in Fig. 1. The external heat input at the evaporator causes the working fluid to be evaporated. The saturated vapor evaporated at the evaporator flows down to the condenser due to the pressure gradient in the vapor space and then condenses at the inclined surface of the condenser while releasing latent heat. The condensate is returned to the evaporator along the inclined surface by the centrifugal force. While heat energy is transported from the evaporator to the condenser by using the phase change of the working fluid, the working fluid in different phases is being circulated between the evaporator and the condenser.

The purpose of this paper is to introduce a simple analytical method to be used to predict the performance characteristics of rotating heat pipes. The most previous studies assumed that the temperature variation in the condensate is linear and the inertia term in Navier-Stokes equation is negligible [3,4,5,6]. In this study, the temperature and velocity distribution in the condensate are obtained by solving the Navier-Stokes and energy equations to consider their effects. The heat transfer rate of the rotating heat pipe is presented for the variations of the angular velocity, taper angle, and working fluid.

2. Analysis

For a simple analysis, the condensate is assumed to be incompressible, constant property fluid. The flow of the condensate is laminar and film condensation takes place

at the surface of the condenser. The friction at the liquid-vapor interface is negligible. The vapor in the vapor space is saturated at saturation temperature T_s and there is no condensable gas. The angular velocity is large enough for the gravity force to be omitted. The surface temperature at the condenser is uniform temperature T_w .

Governing Equations and Transformation

For the physical system shown in Fig. 1, the equations for conservation of mass, momentum, and energy can be expressed as follows

$$\frac{\partial V_x}{\partial x} + \frac{V_x}{x} + \frac{\partial V_y}{\partial y} = 0 \quad (1)$$

$$V_x \frac{\partial V_x}{\partial x} + V_y \frac{\partial V_x}{\partial y} - \frac{V_\phi^2}{x} = \nu \frac{\partial^2 V_x}{\partial y^2} \quad (2)$$

$$V_x \frac{\partial V_\phi}{\partial x} + V_y \frac{\partial V_\phi}{\partial y} + \frac{V_x V_\phi}{x} = \nu \frac{\partial^2 V_\phi}{\partial y^2} \quad (3)$$

$$V_x \frac{\partial V_y}{\partial x} + V_y \frac{\partial V_y}{\partial y} = -\frac{1}{\rho} \frac{\partial P}{\partial y} + \nu \frac{\partial^2 V_y}{\partial y^2} \quad (4)$$

$$V_x \frac{\partial T}{\partial x} + V_y \frac{\partial T}{\partial y} = \alpha \frac{\partial^2 T}{\partial y^2} \quad (5)$$

Instead of solving these partial differential equations, we may transform them to a set of ordinary differential equations that are easier to solve using new variables. For this purpose, some important assumptions are made. First, the system is axis symmetric, i.e., $\partial/\partial\phi=0$. Second is that the velocity and the temperature profiles do not change shape in the x-direction. This implies that the temperature distribution depends only on y (and hence η) and the condensate thickness may be uniform over the surface. With these assumptions, new variables are defined as follows

a) new independent variable

$$\eta = y \sqrt{\frac{\omega \sin \alpha}{\nu}} \quad (6)$$

b) new dependent variables

$$F(\eta) = \frac{V_x}{x\omega \sin \alpha}, \quad G(\eta) = \frac{V_\phi}{x\omega \sin \alpha}, \quad H(\eta) = \frac{V_y}{\sqrt{\omega v \sin \alpha}},$$

$$\theta(\eta) = \frac{T_{sat} - T}{T_{sat} - T_w}, \quad P(\eta) = \frac{P}{\mu\omega \sin \alpha} \quad (7)$$

Results of transformation of equations (1-5) become

$$H' = -2F \quad (8)$$

$$F'' = HF' + F^2 - G^2 \quad (9)$$

$$G'' = HG' + 2FG \quad (10)$$

$$P' = H'' - HH' \quad (11)$$

$$\theta'' = (\text{Pr})H\theta' \quad (12)$$

The primes denote differentiation with respect to η and Pr represents the Prandtl number. Combining equation (8), (9), and (10) gives

$$H'' = (HH' - (H')^2)/2 + 2G^2 \quad (13)$$

$$G'' = HG' - H'G \quad (14)$$

Boundary conditions

To obtain specific solutions, the boundary conditions are needed at the wall surface and the liquid-vapor interface. At the wall surface, no slip condition is used and the temperature of the liquid immediately adjacent to the wall is the same as that of the wall temperature T_w . At the liquid-vapor interface, there is negligible shear and the condensate and vapor have the common saturation temperature T_s . These boundary conditions are

$$y=0(\text{wall surface}) \begin{cases} V_x = 0 \\ V_\phi = x \sin \alpha \omega \\ V_y = 0 \\ T = T_w \end{cases} \quad y=\delta(\text{liquid-vapor interface}) \begin{cases} \tau_{yx} = 0 \\ \tau_{y\phi} = 0 \\ T = T_{sat} \end{cases} \quad (15)$$

By using the same independent and dependent variables, the boundary conditions are transformed as follows

$$\eta = 0 \text{ (wall surface)} \begin{cases} H=0 \\ H'=0 \\ G=1 \\ \theta=0 \end{cases} \quad \eta = \eta_\delta \text{ (liquid-vapor interface)} \begin{cases} H''=0 \\ G'=0 \\ \theta=0 \end{cases} \quad (16)$$

To relate η_δ (and condensate thickness δ) to known physical quantities, an over-all energy balance may be expressed as follows

$$h_{fg} \int_0^\delta \rho 2\pi x \sin \alpha V_x dy + \int_0^\delta \rho 2\pi x \sin \alpha V_x C_p (T_{sat} - T) dy = \pi x^2 \sin \alpha k \left(\frac{\partial T}{\partial y} \right)_{y=0} \quad (17)$$

By using new variables defined the over-all energy balance becomes

$$\frac{C_p \Delta T}{h_{fg}} = Pr \cdot \left[\frac{H}{\theta'} \right]_{\eta_s} \quad (18)$$

Our prime interest is the temperature distribution and the heat transfer, and hence the solution of equation (12) should be obtained. However in equation (12), θ is intimately connected with velocity functions H and G through equation (12), (13), and (14). Simultaneous solutions of H and G are needed for integration of equation (12) for the temperature distribution. Numerical solutions of equations (12), (13), and (14) subjects to the boundary conditions (16) have been carried out using the Runge-Kutter method for several Pr numbers. Also equation (18) is solved to obtain the condensate thickness.

3. Results and Discussions

The rotating heat pipe may continuously perform when adequate amount of the condensate returns to the evaporator. Thus it is very important to inspect the velocity distributions across the condensate although in this study dry-out of the condensate cannot be predicted. We select a representative situation that has the dimension-less layer thickness of 5.0 to typify thick film. Figure 2 shows the distribution of each velocity component across the condensate film. The tangential velocity V_ϕ that is the maximum at the surface of the condenser decreases significantly across the layer. Also significant amount of mass transfer toward the surface of the condenser from the liquid-vapor interface can be seen from the velocity component V_y . The velocity in the x-direction increases from zero to the maximum and then gradually decreases.

Figure 3 shows the temperature distributions across the condensate for Pr=10 for

high Pr number working fluids. The profiles are almost a straight line for several values of $C_p \Delta T / H_{fg}$. Thus the most heat transfer rate across the condensate may be carried by the conduction heat transfer. From these results, we may expect that the temperature profile for low Pr number working fluids is even linear.

To study the effects of major design factors such as the angular velocity, the taper angle of the condenser surface, and the working fluids, a specific dimension of a rotating heat pipe is chosen. The length of the condenser is 23.3cm and the taper angle is 5° . Water is used for the working fluid. Figure 4 shows the effect of the angular velocity on the heat transport capability of the rotating heat pipe. For a given working fluid, the heat transfer rate is increased with increasing the angular velocity and the temperature difference between the wall temperature and the saturation temperature. Figure 5 shows that for the same angular velocity the heat transfer is increased with increasing the taper angle. However, the physical condition would limit the increase of the taper angle. Figure 6 shows the effects of the properties of the working fluids such as water, acetone, and Freon-113 that can be used at the same temperature range. Water is superior to two others as working fluid. This implies that the proper selection of the working fluid for the given operating conditions is also very important.

4. Concluding Remarks

The performance characteristics of the rotating heat pipe are analytically studied. The temperature distribution across the condensate is linear and the conduction is the major heat transfer mode. The properties of the working fluid, the rotating speed, and the taper angle greatly affect the performance of the rotating heat pipe. The analytical results show that the increase in the rotating speed and the taper angle enhances the heat transport capability.

Acknowledge

This work was supported from the Electrical Engineering & Science Research Institute in the Republic of Korea. This paper was also presented at the 1st Korea-Russia International Symposium on Science and Technology, Ulsan Korea, 1997.

References

1. S. W. Chi, *Heat Pipe Theory and Practice*, 1976, Hemisphere Publ.
2. P. D. Dunn and D. A. Reay, *Heat Pipes*, 1982, Pergamon Publ.
3. T. C. Diniels and F. K. Al-Jumaily, *Int. J. Heat and Mass Transfer*, 1975, 18, pp. 961-973.
4. T. C. Diniels and F. K. Al-Jumaily, *Proc. 1st Int. Heat Pipe Conf.*, 1973
5. T. C. Diniels and R. J. Williams, *Int. J. Heat and Mass Transfer*, 1978, 21, pp. 193-201.
6. T. C. Diniels and F. K. Al-Jumaily, *Int. J. Heat and Mass Transfer*, 1979, 22, pp. 1237-1241.

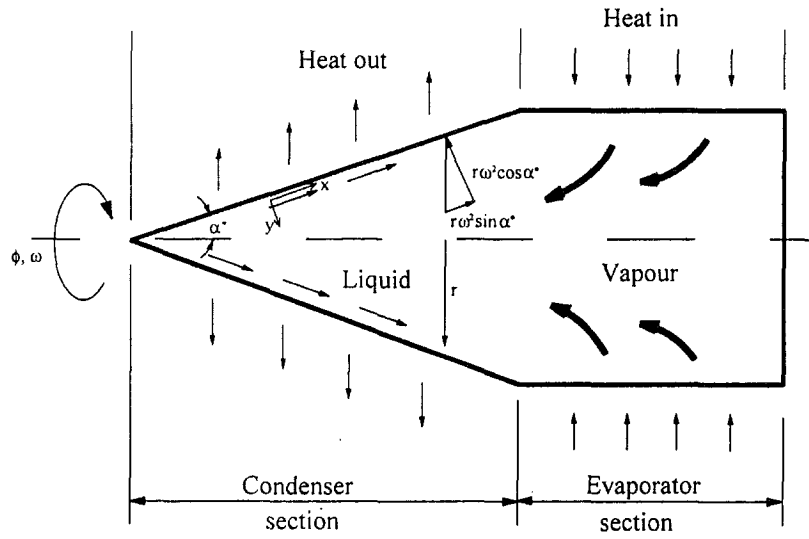
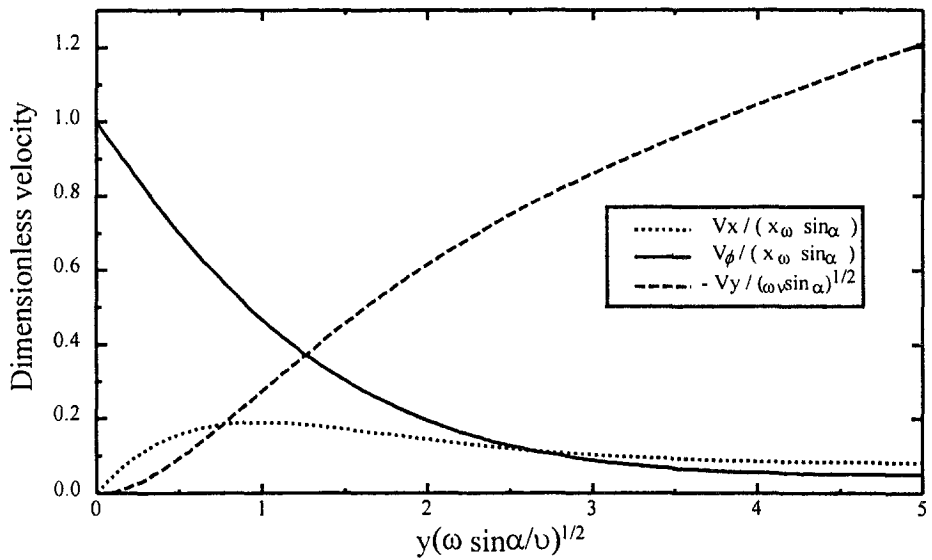


Fig. 1 Schematic diagram of the physical system

Fig. 2 Velocity distributions for $\delta (\omega \sin\alpha/v)^{1/2} = 5$

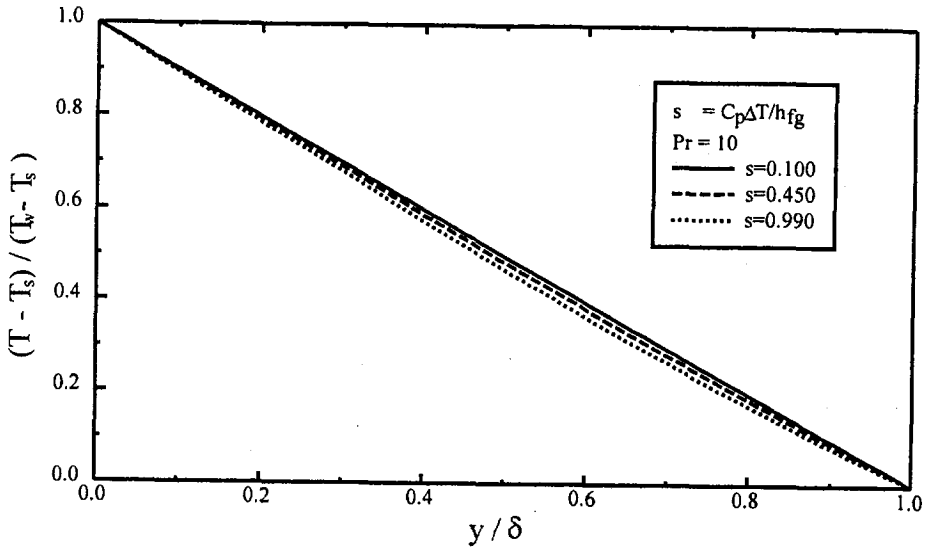


Fig. 3 Temperature distributions across condensate layer for $Pr = 10$

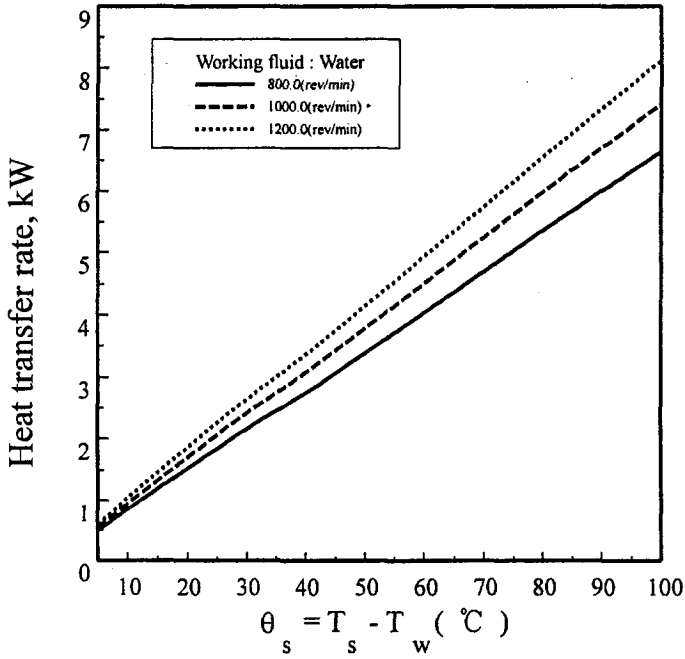


Fig. 4 Heat transfer rate Q versus θ_s for various speeds

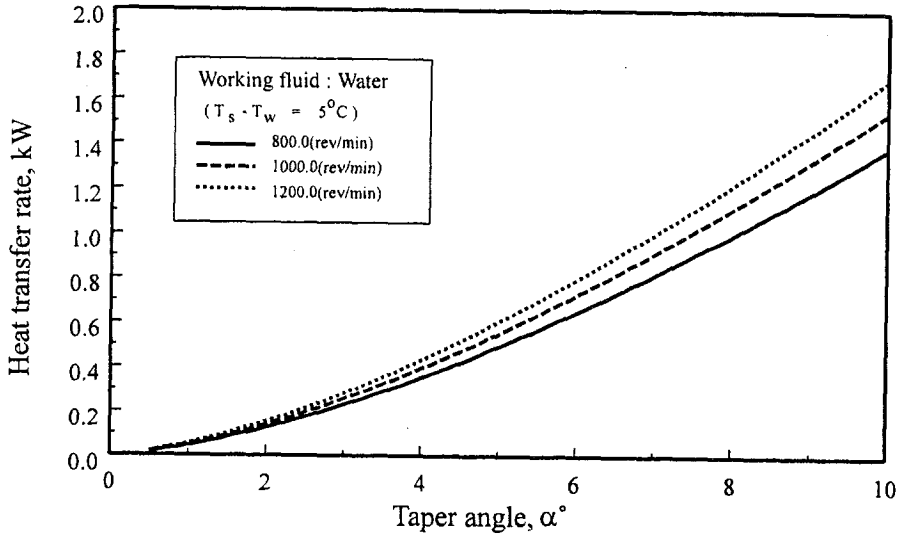


Fig. 5 Effect of taper angle

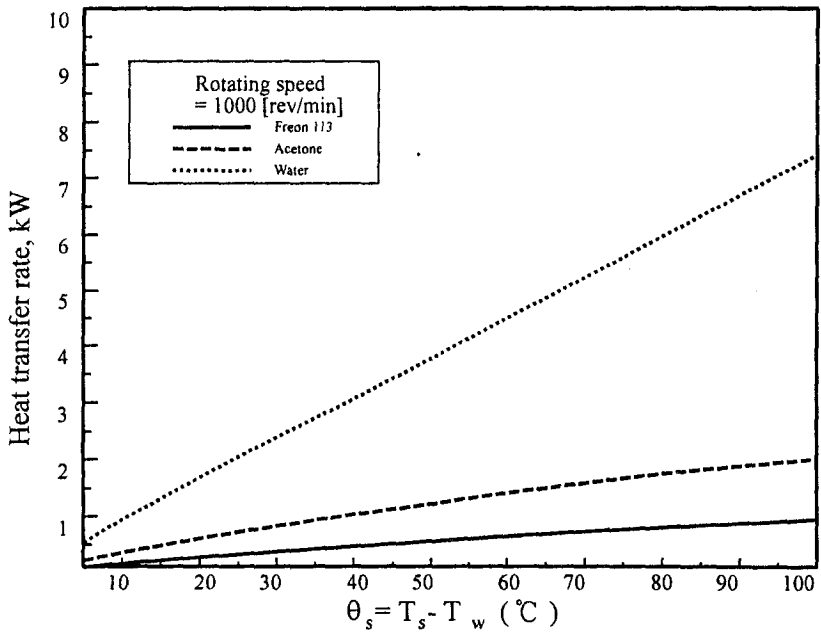


Fig. 6 Heat transfer rate Q versus θ_s for various working fluids